

Special optical geometry for measuring twist elastic module K_{22} and rotational viscosity γ_1 of nematic liquid crystals

A. V. Dubtsov,¹ S. V. Pasechnik,^{1,2} D. V. Shmeliova,¹ V. A. Tsvetkov,¹ and V. G. Chigrinov^{2,a)}

¹Moscow State University of Instrument Engineering and Computer Science, Stromynka 20, Moscow 107996, Russia

²Hong Kong University of Science and Technology, Clear Water Bay, Kowloon, Hong Kong

(Received 25 December 2008; accepted 2 April 2009; published online 6 May 2009)

A special nontraditional optical geometry with a pure twist deformation induced by a homogeneous “in-plane” electric field in the layer of nematic liquid crystal (LC) is presented. A quantitative agreement of the theoretical and experimental results of the measured LC birefringence is obtained. A method for measuring the twist elastic module K_{22} and the rotational viscosity coefficient γ_1 of nematic LC is proposed. © 2009 American Institute of Physics. [DOI: 10.1063/1.3129864]

Viscous-elastic properties of nematic liquid crystal (LC) define the static and dynamic technical characteristics of LC devices. In particular, the threshold voltage and the transmission-voltage characteristic is obtained using Frank’s elastic modules K_{11} , K_{22} , and K_{33} , whereas the switching times may depend, in general, on different combinations of dissipative Leslie’s coefficients. In most practically important cases the switching times are proportional to the rotational viscosity coefficient γ_1 , which plays the key role in LC dynamic behavior.¹

It is well known that a measurement of LC twist elastic constant K_{22} is much more difficult than the splay K_{11} and bend K_{33} modules. The conventional Fréedericksz transition technique is not effective in this case as a registration of field induced changes of a twist angle is possible only via a conoscopic observation in the traditional optical geometry.² The corresponding rotation of conoscopic images is not sensitive to the orientational deformations as in the case of birefringence measurements used in the determination of K_{11} and K_{33} . An alternative light-scattering method³ requires a delicate adjustment of the optical system. Thus, the variation in the measured K_{22} values is rather high even in the case of well-studied LC like 5CB. Various K_{22} values were found in the range of 3×10^{-12} N... 6.2×10^{-12} N.⁴⁻⁶ The more reliable results with an accuracy of $\pm 7\%$ were obtained using four independent light-scattering techniques.⁷

Several different techniques were proposed to determine the LC rotational viscosity coefficient γ_1 .⁸⁻¹¹ Direct measurements of a mechanical moment induced in bulk LC samples by rotating magnetic fields provide the best accuracy in γ_1 measurement.⁸ However, strong magnetic fields, an appearance of defects, and a large LC amount used in this method considerably restrict its application. Thus, it is highly desirable to extract the LC rotational viscosity coefficient directly from the experiments with thin LC layers. Unfortunately, backflow effects cause a substantial contribution to the effective value of γ_1 in most LC thin layer geometries. Only a pure LC twist deformation mentioned above does not induce a motion of LC molecular mass and the backflow effects do not take place. A conoscopic observation of such a

type of LC deformation in a magnetic field was proposed previously to measure γ_1 value.^{10,11}

Recently we revealed a special nontraditional geometry for the study of both static and dynamic properties of LC layers, confined by the surfaces with different anchoring strengths.¹² The key advantages of the LC cell are very high sensitivity of an optical response to the small variations in the twist angle and the possibility to apply a homogeneous “in-plane” electric field. Two pairs of transparent glass substrates were formed to realize a narrow channel of a rectangular cross section (Fig. 1). It gives an opportunity to observe LC director orientation in both x and z directions. The top and bottom surfaces were treated in a standard manner to provide a homeotropic orientation and to avoid defects of the LC orientation. The inner polished edges were treated by photoalignment technology based on UV illumination of an azo dye (SD1, Dainippon Ink and Chemicals¹³). It provided well-defined planar boundary orientation with various values of the LC anchoring strength W controlled by different UV irradiation D_p doses. Two types of the LC cells [with non-symmetric, Fig. 1(b), and symmetric, Fig. 1(c), boundary conditions] were used to investigate a pure twist deformation.

The cells were filled by nematic liquid crystals with positive values of LC dielectric anisotropy $\Delta\epsilon$ (5CB from Merck for the first cell and nematic mixture ZhK 616 from

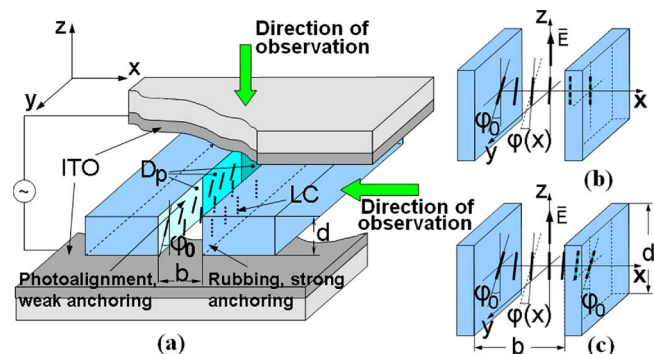


FIG. 1. (Color online) (a) General scheme of LC cell and the distribution of NLC director orientation in (b) the channel with nonsymmetric and (c) symmetric boundary conditions: b) $\varphi_0=25^\circ$, $b=62 \mu\text{m}$, and $d=270 \mu\text{m}$ (5CB); c) $\varphi_0=21^\circ$, $b=130 \mu\text{m}$, and $d=1 \text{ mm}$ (LC 616).

^{a)}Electronic mail: eechigr@ust.hk.

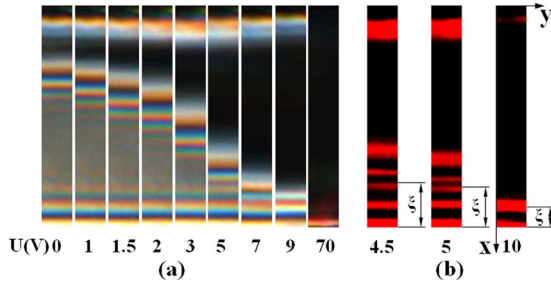


FIG. 2. (Color online) Microscopic images of the channel in the cell with nonsymmetrical boundary conditions at different voltages obtained from z direction [Figs. 1(a) and 1(b)]: a) in a natural light and b) in a red color after image processing. The images were made at the temperature of 25 °C.

NIOPIK for the second cell). A homogeneous “in-plane” electric field ($f=3$ kHz) was applied to the electrodes along z direction to produce twistlike deformation of LC director. An observation of the cells from x direction does not reveal strong variations in light intensity due to the waveguide Mauguin regime of light propagation in the LC layer.¹ At the same time the strong birefringence of a polarized light propagating through the rectangular LC cell along z direction was registered via an appearance of interference stripes. These stripes (Fig. 2) can change their position after an application of very weak electric fields (about 0.002 V/ μm) to LC layer in z direction.

The dependence of the azimuthal angle $\varphi(x)$ of a director rotation [Fig. 1(b)] in a quasistatic regime under the action of the electric field can be easily obtained from the basic equations¹⁴ taking into account a finite value of the surface anchoring,

$$\varphi(x) = C \text{sh}(\xi^{-1}x), \quad (1)$$

where

$$C = \frac{\varphi_0 \xi}{L_s \text{ch}(\xi^{-1}b) + \xi \text{sh}(\xi^{-1}b)}, \quad (2)$$

and

$$\xi = \frac{1}{E} \left(\frac{K_{22}}{\varepsilon_0 \Delta \varepsilon} \right)^{1/2}, \quad (3)$$

where $E=U/d$ is the electric field strength, $\Delta \varepsilon$ is the dielectric anisotropy, and L_s is the extrapolation length related to LC anchoring strength W ,

$$L_s = K_{22}/W. \quad (4)$$

The phase delay δ between the ordinary and extraordinary rays propagated in z direction can be written as

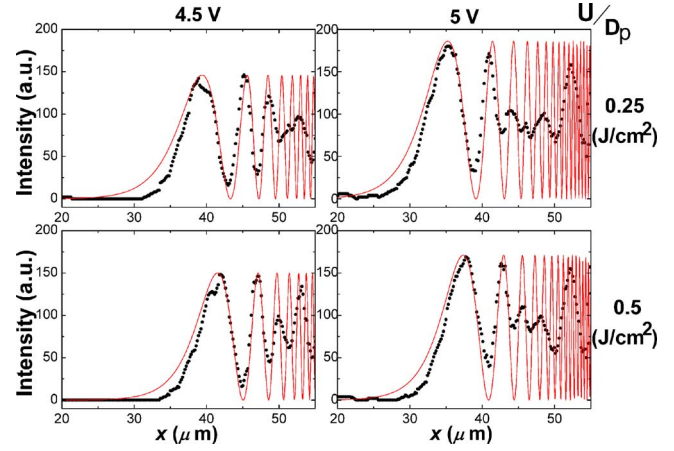


FIG. 3. (Color online) Dependence of the light intensity $I(x)$ obtained after image processing [blue color extracted from Fig. 2(a)]; solid curve—approximation line at parameters $\Delta \varepsilon=11.5$, $\Delta n=0.21$, $\lambda=462$ nm, and $\varphi_0=25^\circ$.

$$\delta = \frac{2\pi d \Delta n}{\lambda} \sin^2 \varphi(x,t) \approx \frac{2\pi d \Delta n}{\lambda} [\varphi(x,t)]^2, \quad (5)$$

where Δn is the optical anisotropy, d is the thickness of the cell, and λ is the wavelength.

The obtained equation explains the interference picture and its variation with increasing voltage as for our geometry, δ defines intensity of polarized light $I(x,t)$ passing in the z direction,

$$I(x,t) = I_0 \sin^2 \frac{\delta(x,t)}{2}. \quad (6)$$

For a stationary case the coordinates x_m and x_n of the interference maxima (minima) of different orders (m,n) write

$$\frac{\text{sh}^2(\xi^{-1}x_m^{\max})}{\text{sh}^2(\xi^{-1}x_n^{\max})} = \frac{2m-1}{2n-1}, \quad \frac{\text{sh}^2(\xi^{-1}x_m^{\min})}{\text{sh}^2(\xi^{-1}x_n^{\min})} = \frac{m}{n}, \quad (7)$$

where $m,n=1,2,3,\dots$ is the order of the maximum or minimum, defined by Eq. (7).

The Eqs. (7) and (3) can be used to determine the LC electric coherence length ξ and the ratio $K_{22}/\Delta \varepsilon$. Thus, the Frank’s elastic module K_{22} can be calculated using the known values of LC dielectric anisotropy $\Delta \varepsilon$.

Table I demonstrates an example of such calculations. A comparison between the experimental data and theoretical $I(x)$ dependences is shown in Fig. 3.

The symmetric boundary conditions and special parameters of the channel with a relatively small angle φ_0 of the

TABLE I. Calculated values of ξ , K_{22} , and W ($W=15 \times 10^{-6}$ J/m² correspond to $D_p=0.5$ J/cm²) (Ref. 15). An average value of $K_{22}=(3.5 \pm 0.4)10^{-12}$ N is in accordance with independent measurements.

D_p J/cm ²	x_1^{\max}, x_1^{\min}	x_1^{\max}, x_1^{\min}		x_1^{\max}, x_2^{\max}		x_1^{\min}, x_2^{\min}		ξ (μm)
		$K_{22}/\Delta \varepsilon \times 10^{-13}, N$	$K_{22} \times 10^{-12}, N$	$K_{22}/\Delta \varepsilon \times 10^{-13}, N$	$K_{22} \times 10^{-12}, N$	$K_{22}/\Delta \varepsilon \times 10^{-13}, N$	$K_{22} \times 10^{-12}, N$	
0.25 (7)	4.5	2.9	3.3	3.1	3.6	3.3	3.8	11.3
	5	3.1	3.5	3.0	3.4	3.5	3.9	10.2
0.5 (15)	4.5	3.9	3.3	2.7	3.1	3.4	3.9	
	5	3.0	3.5	2.9	3.4	3.2	3.7	

TABLE II. Time coordinates of interferential maximum (t_m^{\max}) or minimum (t_n^{\min}) at different x and the calculated values of γ_1 .

x (μm)	γ_1, P						γ_{1av}, P
	t_2^{\max}, t_1^{\max}	t_3^{\max}, t_2^{\max}	t_3^{\max}, t_1^{\max}	t_2^{\min}, t_1^{\min}	t_2^{\min}, t_2^{\max}	t_3^{\min}, t_2^{\max}	
28	2.36	2.3	2.33	2.36	2.31	2.31	2.36
24	2.59	2.13	2.38	2.45	2.23	2.21	
18	2.47	2.28	2.38	2.49	2.67	2.21	

second cell tend to a linear regime of a director motion after switching off the electric field. It results in a slow variation in the interference stripes.

After switching off the voltage, the electric-field torque becomes zero. At the final stage of the relaxation process the slowest harmonic with time,¹⁶

$$\tau_0 = \frac{\gamma_1 b^2}{K_{22} \pi^2}, \quad (8)$$

which defines the dynamics of the LC director reorientation. The corresponding variations in the azimuthal angle are expressed as

$$\varphi(x, t) = \varphi_0 - \varphi(0) \exp\left(-\frac{t}{\tau_0}\right) \cos \frac{\pi x}{b}. \quad (9)$$

The latter equation together with Eqs. (5) and (6) can be used for fitting the time variations in the interference stripes, which makes possible to determine the relaxation time τ_0 .

If an LC phase delay is large enough, we can obtain the relaxation time τ_0 and the rotational viscosity coefficient γ_1 (using the value of K_{22}) by measuring the intervals between time coordinates t_m^{\max} and t_n^{\min} corresponding to interferential maxima or minima,

$$\tau_0 = \frac{t_m - t_n}{\ln \frac{\sqrt{\delta_m} - \sqrt{B\varphi_0}}{\sqrt{\delta_n} - \sqrt{B\varphi_0}}}, \quad (10)$$

where $B = 2\pi d \Delta n / \lambda$, t_m and t_n are the time coordinates of extremes, $\delta_m[\delta_n] = 2\pi m[2\pi n]$ for maxima, and $\delta_m[\delta_n] = 2\pi(m-1)[2\pi(n-1)]$ for minima.

The results of such calculations are presented in Table II. The average value of the rotational viscosity coefficient γ_1 is in agreement with the previously obtained results.¹⁷

In conclusion, we proposed a nontraditional method for determination of LC twist elastic module K_{22} and rotational viscosity coefficient γ_1 using an electrically induced pure twist deformation. The specific choice of the direction of an observation makes it possible to use LC optical birefringence data only without any conoscopic or light-scattering mea-

surements. The rotational viscosity coefficient γ_1 and Frank's twist elastic module K_{22} can be determined by analyzing the digital images obtained in the specific optical geometry. The proposed method is simple and can be effectively used for measurements of LC parameters.

This work was partially supported by RF President Scholarship (Grant No. RFBR 06-02-16287) to study abroad, Program of RF Ministry of Education (Grant No. 2.1.1/5873), and HKUST (Grant Nos. CERG 612 208 and CERG RPC07/08.EG01).

¹L. M. Blinov and V. G. Chigrinov, *Electrooptic Effects in Liquid Crystal Materials* (Springer, New York, 1994).

²P. Oswald and P. Pieranski, *Nematic and Cholesteric Liquid Crystals: Concepts and Physical Properties Illustrated by Experiment* (CRC, Boca Raton, 2005).

³G.-P. Chen, H. Takezoe, and A. Fukuda, *Jpn. J. Appl. Phys., Part 1* **28**, 56 (1989).

⁴R. Stannarius, in *Handbook of Liquid Crystals*, edited by D. Demus, J. Goodby, G. W. Gray, H.-W. Spiess, and V. Vill (Wiley, Weinheim, 1998), pp. 60–84.

⁵D. A. Dunmur, *Physical Properties of Liquid Crystals: Nematics*, edited by D. Dunmur, A. Fukuda, and G. Luckhurst (INSPEC, London, 2001), pp. 216–229.

⁶M. Cui and J. R. Kelly, *Mol. Cryst. Liq. Cryst.* **331**, 49 (1999).

⁷T. Toyooka, G. Chen, H. Takezoe, and A. Fukuda, *Jpn. J. Appl. Phys., Part 1* **26**, 1959 (1987).

⁸H. Knepe and F. Schneider, *J. Phys. E* **16**, 512 (1983).

⁹F.-J. Bock, H. Knepe, and F. Schneider, *Liq. Cryst.* **1**, 239 (1986).

¹⁰P. E. Cladis, *Phys. Rev. Lett.* **28**, 1629 (1972).

¹¹F. Leenhouts and A. J. Dekker, *J. Chem. Phys.* **74**, 1956 (1981).

¹²S. V. Pasechnik, D. V. Shmeliova, V. A. Tsvetkov, A. V. Dubtsov, and V. G. Chigrinov, *Mol. Cryst. Liq. Cryst.* **479**, 59 (2007).

¹³V. G. Chigrinov, V. M. Kozenkov, and H.-S. Kwok, *Photoalignment of Liquid Crystalline Materials: Physics and Applications* (Wiley, New York, 2008).

¹⁴S. V. Pasechnik, V. G. Chigrinov, D. V. Shmeliova, V. A. Tsvetkov, V. N. Kremenetsky, L. Zhijian, and A. V. Dubtsov, *Liq. Cryst.* **33**, 175 (2006).

¹⁵X. Lu, F. K. Lee, P. Sheng, H. S. Kwok, V. Chigrinov, and O. K. C. Tsui, *Appl. Phys. Lett.* **88**, 243508 (2006).

¹⁶P. G. de Gennes, *The Physics of Liquid Crystals* (Clarendon, Oxford, 1974).

¹⁷A. N. Larionov, N. N. Larionova, and S. V. Pasechnik, *Mol. Cryst. Liq. Cryst.* **409**, 459 (2004).